



Ag@SnO₂@ZnO core-shell nanocomposites assisted solar-photocatalysis downregulates multidrug resistance in *Bacillus* sp.: A catalytic approach to impede antibiotic resistance



Sourav Das^{a,b,1}, Ananya Jyoti Misra^{a,b}, A.P. Habeeb Rahman^{a,b}, Bhaskar Das^c, R. Jayabalan^c, Ashok J. Tamhankar^{b,d}, Amrita Mishra^b, Cecilia Stålsby Lundborg^{d,2}, Suraj K. Tripathy^{a,b,*,2}

^a School of Chemical Technology, Kalinga Institute of Industrial Technology (KIIT), Bhubaneswar, India

^b School of Biotechnology, Kalinga Institute of Industrial Technology (KIIT), Bhubaneswar, India

^c Department of Life Sciences, National Institute of Technology, Rourkela, India

^d Department of Public Health Sciences, Karolinska Institutet, Stockholm, Sweden

ARTICLE INFO

Keywords:

Antibiotics

Core-shell

Multidrug resistance

Nanocomposites

Photocatalysis

ABSTRACT

In the present study, we report the solar-photocatalytic disinfection (SPCD) of a multidrug resistant (MDR) bacterium, *Bacillus* sp. CBEL-1 using Ag@SnO₂@ZnO core-shell nanocomposites (NCs) as catalyst. Complete disinfection was observed within 210 min with a catalyst concentration of 500 mg/L when subjected to NCs mediated PCD under solar irradiation. H₂O₂ was found to be the key reactive oxygen species (ROS) involved in SPCD of targeted bacteria. Increase in production of 4-HNE along with change in fatty acid profile of bacteria after SPCD induced oxidative stress indicates the compromisation of bacterial cell membrane. Irreversible change in antibiotic resistance profile of the target bacteria was notice after SPCD, without recovery even after 96 h post disinfection experiments. Traditional disinfectants and UV-250 nm were found to have marginal impact on the resistance profile of the bacteria compared to that of SPCD. Disinfection achieved using the NCs were also validated for real water samples.

1. Introduction

In the United Nations (UN) millennium development goals, right to clean water has been manifested as one of the fundamental need of human life [1]. Scarcity of safe drinking water and proper hygienic practices is known to have pernicious health impact afflicting a large population, particularly those living in low and middle income countries [2–4]. Water borne diarrhoeal diseases which usually are caused by ingestion of water infected with pathogens are accountable for nearly 2 million deaths worldwide with major risks to children below the age of five [5,6]. In India alone, over the last five years approximately 10,738 deaths have been reported due to illness related to water [7]. Amongst various pathogenic microorganisms, members of the bacterial genus *Bacillus* (*Bacillus* sp.) have been recognized as opportunistic pathogen and could be a causative agent of local infections (particularly of burns, traumatic or postsurgical wounds, and the eye),

bacteremia and septicemia, meningitis, respiratory infections, endocarditis and pericarditis, and food poisoning [8,9]. In coming years it is expected that the infections related to *Bacillus* sp. is likely to increase in neonates [10], intravenous drug users [11], the immunologically compromised, including patients with AIDS and malignant disease [8], and those with artificial prostheses, including orthopedic implants and cerebrospinal shunts [12]. Being ubiquitous in the nature, these bacteria can survive in varieties of environmental conditions. Water and food sources are particularly known to be the major channel through which transmission of *Bacillus* sp. may spread [13]. These bacteria have ability to survive under harsh environmental conditions and hence may pass through the community level water treatment processes [14]. Recently the situation has become more harrowing because of development of multi-drug resistant (MDR) *Bacillus* sp. [15,16]. India from 2000 to 2015 has doubled its antibiotic dependency and use with a shot upto 103%, promoting strokes of increase in antimicrobial resistance

* Corresponding author.

E-mail address: suraj.tripathy@kiitbiotech.ac.in (S.K. Tripathy).

¹ Present address: National Innovation Foundation-India (Bhubaneswar Cell), An Autonomous Body of the Department of Science and Technology, Government of India.

² Authors have equal contribution to the study.

(AMR) [17]. AMR is a relentless phenomenon exerted by microbes to nullify the effect of antibiotics. Several of the mechanisms to achieve this include formation of more efflux pumps, active site modification, production of antibiotic degrading enzymes etc [18]. Bacteria which confer resistance against at least three groups of antibiotics are usually represented as MDR strains and can not only contaminate the water sources but also may transfer their resistance to naive bacteria by a horizontal gene transfer process [19]. This in turn can significantly compromise the therapeutic potential of presently available antibiotics against pathogens and hence could lead to a serious public health concern [19,20]. Recent WHO report has predicted that AMR menace may kill no less than 10 million people per year [21]. Unfortunately, most of the currently available water treatment techniques not only succumb to the evolving pressure of microbes, but also these water treatment plants itself are becoming a sizeable reservoir for generating AMR [22]. Conventional water treatment techniques like chlorination, iodination, ozonation and UV is diminishing due to their invariably high toxic by-product formation, less favorable reaction economics and energy intensified operation alongside the questionable process efficiency in connection with the regrowth of microbes after treatment [23]. Though separation techniques like reverse osmosis and ultra-filtration may remove the microorganism, to a large extent they are ineffective in deactivating the same [24]. This necessitates immediate and systematic studies for development of new disinfection techniques to minimize the burden of MDR bacteria. In this aspect, sun-light assisted photocatalysis (SPC) has gained much attention in recent times due to its exemplary advantages such as operational intelligibility and cost-effectiveness [24,25]. SPC is an advanced oxidation process (AOP) which involves the action of a semiconductor (e.g. TiO₂, ZnO, SnO₂ etc.) nanoparticle (NP) catalyst under a light of suitable wavelength (including sun-light), resulting in the generation of various reactive oxygen species (ROS) which in turn can be used to kill bacterial cells [25,26]. Fernández-Ibáñez et al. have used TiO₂/graphene composites for SPC inactivation of *E. coli* [27]. Jia and co-workers have reported the disinfection of *E. coli* by SPC using TiO₂-Bi₂WO₆ binanosheet [28]. Mn and Co doped TiO₂ was used by Danae Venieri et al. for SPC disinfection of *E. coli* [29]. JoanneMac Mahon et al. has successfully used TiO₂, ZnO and ruthenium based complexes in a continuous flow system for SPC disinfection of *E. coli* [30]. Most of the initial attempts were focused on the disinfection of normal *E. coli* and systematic study on disinfection of MDR bacteria was lacking. Das et al. for the first time reported the SPC disinfection of MDR *E. coli* using Fe-doped ZnO NPs [31]. To decipher its potential for real world application, SPC assisted disinfection technique has to be validated with other water borne bacterial species. However, ZnO NPs when used for SPC process may involve few operational complexities due to time dependent morphogenesis (e.g. irreversible aggregation, crystal growth or alteration of the surface morphology) which may dwindle its catalytic efficiency and can limit its commercial utilization. To deal with these limitations, researchers have been trying to develop metal/metal oxide nanocomposites (NCs) with core-shell morphology which may preserve the efficiency of the resultant catalyst system in harsh operational environment. Core-shell structure can have advantages over pure metal oxides not only because they offer stability to the metal NPs against harsh reaction conditions but also have shown superior SPC disinfection ability against *Vibrio cholerae* 569B [32]. However, to the best of our knowledge any core-shell NC system has not been investigated for the SPC disinfection of water borne MDR bacteria such as *Bacillus* sp.

Keeping this in view, present study reports Ag@SnO₂@ZnO core-shell NCs based solar-photocatalytic disinfection (SPCD) of MDR *Bacillus* sp. CBEL-1 (Accession Number- SAMN10721426). Core-shell NCs were synthesized via colloidal precipitation technique and used for SPCD experiments. Effect of different reaction parameters on the efficiency disinfection process was investigated and compared with that of other catalysts such as TiO₂ (Degussa P25), ZnO NPs and Ag@ZnO NCs. Lipid peroxidation, DNA and protein leakage studies, resazurin assay

were performed to indicate irreversible compromisation of bacterial cell membrane, metabolism and morphology with simultaneous validation using electron microscopy and fluorescent staining. Additionally, time dependent increase in membrane by-product 4-hydroxy-2-nonenal (4-HNE), which acts as a suicidal molecule synergistically acting on the bacteria for enhancing the rate of disinfection, confirms the disinfection of the targeted bacteria. FAME analysis of the membrane fatty acids was performed to study the change in fatty acid components in response to SPC and oxidative stress. The current study to the best of our knowledge, reports for the first time about deleterious and detrimental effect of the SPCD process on the resistance pattern of the bacteria, which showed substantial down-regulation of antibiotic resistance as compared to traditional chemical based disinfection techniques.

2. Experimental

2.1. Materials

Silver perchlorate hydrate (AgClO₄.xH₂O), sodium borohydride (NaBH₄), and tri sodium citrate dihydrate (C₆H₅Na₃O₇.2H₂O) were procured from Sigma Aldrich Limited, India. Zinc nitrate hexahydrate [Zn(NO₃)₂.6H₂O], sodium hexahydroxostannate (Na₂SnO₃.3H₂O), antibiotics discs, ESBL and growth media (Nutrient Broth and Nutrient Agar) were purchased from HiMedia Laboratories Pvt Ltd, India. All the chemicals which were purchased are of analytical grade and hence used as received without any further purification.

2.2. Synthesis and characterization of photocatalyst

2.2.1. Synthesis of Ag NPs

Ag NPs were synthesized by a chemical reduction technique using NaBH₄ as reductant, trisodium citrate dihydrate as a stabilizer and AgClO₄.H₂O as the source for the silver ion [33]. Distilled water (97 mL) was placed in a 250 mL glass beaker in an ice bath. Under vigorous stirring, 1 mL of silver perchlorate (1 mM) followed by 1 mL of sodium borohydride (100 mM) and 0.885 mL of trisodium citrate (3 mM) were added to the above beaker. Due to the formation of Ag NPs, a transparent bright yellow color was observed immediately. This colloid was kept undisturbed and aged for 1 h at room temperature.

2.2.2. Synthesis of Ag@SnO₂ NCs

The deposition of tin dioxide shell on Ag NPs was achieved by a simple precipitation process [33]. 0.1 mM of NaOH solution was used to increase the pH of the aqueous dispersion of the Ag NPs to \approx 10.5 and the resultant solution was heated upto 80 °C. 10 mL of sodium hexahydroxostannate (40 mM) was added to this solution and the reaction was allowed to stir for 30 min. Then the solution was allowed to cool by a natural process.

2.2.3. Synthesis of Ag@SnO₂@ZnO NCs

2 M of NaOH was added drop-wise to 10 mL of zinc nitrate hexahydrate (10 mM) until a white precipitate of zinc hydroxide is observed. Excessive addition of 2 M NaOH solution is done to dissolve the white precipitate [32]. This solution is diluted to 50 mL and was added to Ag@SnO₂ under vigorous stirring at 90 \pm 5 °C. The solution was allowed to stir at this condition for 2 h followed by vacuum drying at 60 °C (Eppendorf, Concentrator plus-22331, Hamburg) until Ag@SnO₂@ZnO NCs (powdered content) is obtained. To remove the water soluble sodium chloride and other impurities, resultant NCs were washed with de-ionized water (three times). These NCs were dried at 80 °C for 12 h and kept in desiccator for further studies.

2.2.4. Characterization of materials

The morphology of the NCs was studied using transmission electron microscopy (TEM, JEOL-JEM-2010). The crystal phase and surface

functional groups of the NCs was investigated by X-ray diffraction technique (D/Max 2005, Rigaku) and FTIR respectively. Optical properties of the nanomaterials have been investigated by UV/Vis spectrophotometer (Cary 100, Agilent).

2.3. Selection and identification of MDR isolate

Bacterial strain was isolated from a pond located near KIIT, Bhubaneswar, Odisha. Water sample was collected aseptically in sterile 500 mL glass bottles (Schott Duran) from the surface. The labeled samples were properly transported on ice to the laboratory for further analysis. 100 mL of the water sample was filtered through 0.45 µm filter (Millex®-HV, Sterile Filter Unit with Durapore® PVDF Membrane) using a sterile 50 mL syringe. These membranes were aseptically placed on solid plates with appropriate selective media (ESBL Agar, HiMedia) and incubated at 37 °C for 24 h [34,35]. Six colonies were picked and made into pure culture and glycerol stock. Microscopy images of the bacterial colony are shown in Fig. S1 (Supplementary data). Antibiotic susceptibility test for each one these isolates was done using Kirby-Bauer Disc diffusion test as per the Clinical and Laboratory Standards Institute (CLSI) guidelines [36]. The full antibiotic concentrations were selected according to the respective MICs for gram positive bacteria listed in CLSI guidelines [36]. The choice of antibiotics were made keeping in mind that more than three groups are to be explored for getting an MDR bacteria [31,35]. The diameter of inhibition zones was measured in millimeter thrice and the average value was taken. Out of six, one isolate was found resistant to 25 antibiotics (corresponding to groups Aminoglycosides, Chloramphenicol, Cephalosporin, Penicillin, Monobactam, Carbapenems, Quinolones, Macrolides, Glycopeptides, Tetracycline, Rifamycin, Oxazolidinone and Sulphamethoxazole, Supplementary data, Table-S1) and was processed further for genus identification and solar SPCD experiments using Ag@SnO₂@ZnO NCs. The isolated MDR bacteria were found to be form the genus *Bacillus* as identified from the whole genome sequencing. It was submitted to NCBI with the name *Bacillus* sp. CBEL-1 (SBIM00000000; BioSample SAMN10721426, Supplementary Fig. S1) and used further for SPCD experiments.

2.4. Solar-photocatalytic disinfection experiments

The SPCD of *Bacillus* sp. CBEL-1 was conducted under natural sun-light. A digital Luxmeter (R-Tek, digital Luxmeter) was used to measure the corresponding sun-light intensity in all the SPCD experiments. All the experiments were done at 100,000 ± 5000 lx (for sun there is an approximate conversion of 0.0079 W/m² per Lux). The glass equipments used in this study were autoclaved at 121 °C and 15 psi for 20 min prior to use for ensuring sterility [32]. The target bacterial cells were grown in nutrient broth (NB) overnight at 37 °C and 180 rpm to attain a cell count of approximate 10⁸ colony forming units (CFU)/mL. The bacterial culture was then washed thrice with 0.9% normal saline solution (NSS) by centrifugation for 15 min at 5000 rpm, to ensure absence of any extracellular and nutrient medium components. Then the cell pellet was re-suspended in 300 mL of autoclaved 0.9% NSS, so as to achieve a final bacterial density of 1 × 10⁷ CFU/mL [31,34]. The final photocatalyst concentration was taken in between 300 to 700 mg/L and the set up was stirred with a magnetic stirrer throughout the disinfection experiment. Initially the reactor was kept in dark condition for 30 min before being exposed to direct sunlight for achieving proper adsorption-desorption equilibrium [24]. 100 µL of reaction sample were aliquot at regular intervals and the appropriate dilution was spread on nutrient agar (NA) plates and kept incubated at 37 °C for 24 h to determine the viable cell count [37]. The "Photolysis or PL" used in this study meant disinfection without photocatalysts under the sunlight only, and "Dark control or DC" meant to be checking the capability of photocatalysts for disinfection in absence of light [24,31,38]. The post SPCD reactivation of bacteria was assessed for 96 h, where the set up

was kept stirring under dark. Sampling was done every 24 h and plating was done in NA plates to perform viable cell count after incubation at 37 °C for 24 h. Effect of various process parameters (e.g. catalyst loading, experimental controls, intensity of sun-light, initial bacterial load on the SPCD efficiency was investigated. The SPCD efficiency of NCs was compared with other photocatalysts such as ZnO, TiO₂ and Ag@ZnO [32]. Disinfection efficacy of the solar-SPCD process in presence of Ag@SnO₂@ZnO NCs was also compared with conventional disinfectants [e.g. Sodium hypochlorite (Chlorination), Potassium iodide (iodination), Hydrogen peroxide, UV-250 nm, Potassium permanganate]. The concentration of conventional disinfectants used in this study was referred from previously available literatures [39–43]. Unless or otherwise mentioned, all the experiments were performed in triplicates.

2.5. Analysis of peroxidized membrane lipids

Malondialdehyde (MDA), a by-product of peroxidized membrane lipids was used as an indicator for this assay. MDA on reaction with thiobarbituric acid (TBA) forms a pink adduct with lambda max at 532 nm. From the SPCD reaction set up, 2 mL of cell-NCs slurry was collected at regular intervals and quantification of MDA was done using lipid peroxidation assay kit (Sigma-Aldrich) as per the manufacturer's protocol in a micro titer plate reader (EPOCH) [31,44]. The concentration of MDA released was expressed in nM/mg cell dry weight. It has been reported previously about production of 4-hydroxynonenal (HNE) as another biomarker of lipid peroxidation [45]. Analysis of HNE was performed, after treating the samples with acetonitrile solution (Merck) in 1:1 ratio followed by centrifugation at 10,000 rpm for 10 min to separate out HNE from bound proteins into the supernatant phase. Absorbance of HNE was taken at 220 nm to get the time dependent release of HNE in the SPCD system [46].

2.6. Analysis of change in membrane fatty acid components

After SPCD, samples drawn at regular intervals were grown in NA at 37 °C for 24 h. Change in Fatty acid components of the grown bacteria were assessed and compared with untreated bacteria using Gas chromatography fatty acid methyl esters (GC-FAME) profiling according to the method reported by Sasser et al. [37,47].

2.7. Analysis of time dependent loss in metabolic activity

Resazurin assay is a technique to identify any alteration in metabolic activity of bacteria [48]. Active bacterial cells contain oxido-reductase, can reduce purple-blue resazurin into pinkish resorufin. The assay was performed with some modification of the previously reported protocol [49]. To a 96 micro titer plate, 55 µL of sample was added for different SPCD time and its respective controls were added along with 235 µL of NB and 10 µL of resazurin (0.675% in DW). The plate was incubated for 48 h at 37 °C to analyze any color change [37]. Photographs were taken at regular intervals.

2.8. Time dependent release of cellular components

SPCD since long has been reported to permeabilize the bacterial membrane followed by subsequent release of cellular bio-molecules mainly DNA and protein in the slurry system. Slurry samples were collected at regular and subjected to low speed centrifugation to remove the photocatalysts. The supernatant fraction was quantified using UV/Vis spectrophotometer (Agilent, Cary 100) to analyze leaked DNA and protein content [50–52].

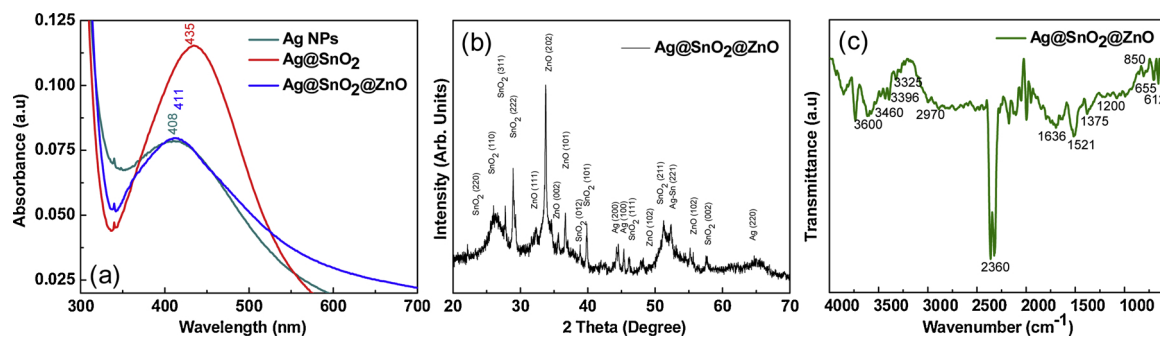


Fig. 1. (a) UV-vis spectrum, (b) XRD pattern and (c) FTIR spectrum of Ag@SnO₂@ZnO NCs.

2.9. Investigation of the bacterial cell membrane damage by Live/Dead staining

The time dependent compromization in bacterial cell membrane was determined using fluorescence microscope. 2 mL of the SPCD reaction slurry and controls were collected at regular intervals, centrifuged and the pellets were washed with 0.9% NSS. Staining of the pellets was done using LIVE/DEAD® BacLight™ (Life Technologies Inc., USA) bacterial viability kit as per the manufacturer's protocol. After incubation in RT for 15 min at dark, the stained samples were observed under Fluorescence Microscope (Floid Cell Imaging Station, Life Technology Inc., USA) at 40 × magnifications. Intact Bacterial cells with unharmed cell membrane (live) are stained by SYTO9 as fluorescent green whereas compromised bacterial cells are stained by propidium iodide as red [31,37,44].

2.10. Analysis of bacterial membrane damage by electron microscopy

2 mL of the SPCD reaction slurry and controls were collected after the respective treatment time. They were subjected to centrifugation and the pellets were washed twice with 0.9% NSS. 50 µL of the pellet dissolved in 0.9%NSS was spread on a clear glass slides and observed under FESEM (NovaTM NanoSEM 450) after glutaraldehyde fixation and ethanol dehydration [53,54].

2.11. Detection of primary reactive oxygen species involved in SPCD

Semiconductor photocatalysis involves in situ generation of different ROSs mainly H₂O₂, O₂⁻, ·OH, h⁺, and e⁻ which are scavenged by EDTA-Fe(II) (100 µM), 4-hydroxy-2,2,6,6-tetramethylpiperidinyloxy (TEMPO) (2 mM), 2-propanol (0.5 mM), Na₂C₂O₄ (0.5 mM), Cr(VI) (50 µM) respectively. To determine the primary ROS involved in the SPCD of *Bacillus* sp. CBEL-1, individual ROS scavengers were employed and time dependent viable bacterial cell count was performed as per the protocol mentioned earlier. The change in disinfection kinetics was compared with the untreated controls to track the primary ROS involved [31,53].

2.12. Stability of the photocatalyst

The stability of the photocatalyst in post reaction condition was investigated using XRD. Water sample subjected to solar-SPCD using Ag@SnO₂@ZnO NCs was analyzed using MP-AES to detect the presence of Ag⁺, Sn²⁺ and Zn²⁺ ions [31].

2.13. Investigation of efficiency of solar-SPCD in real water samples

1 L samples each from pond, river, lake and DI were collected in amber bottles and stored at 4 °C. After filtration using Nylon membrane filter and autoclaving, these water samples were spiked independently with 10⁷ CFU/mL of *Bacillus* sp. CBEL-1. Steps similar to solar-SPCD

regarding sampling, plating in NA, incubation and viable cell count were followed to get the rate of disinfection in different water matrix [31,32,38].

2.14. Assessing the antibiotic resistance pattern after disinfection

Antibiotic resistant and sensitive phenotypes prior to and after disinfection were tested by Kirby-Bauer disk diffusion method according to standard CLSI guidelines [35]. Briefly, treated *Bacillus* sp. CBEL-1 colonies were randomly collected from the final experimental time-point, prior to complete disinfection from the NA plates and after reactivation (if any), transferred into a physiological solution to obtain 10⁸ CFU/mL (0.5 McFarland) suspension. Then it was spread onto NA plates with sterile cotton swab. 27 different antibiotic discs at a frequency of 4 discs per plate were placed gently on the surface of previously swabbed NA plates. After 18 h of incubation at 37 °C, the zone of inhibition for the respective antibiotics were measured and compared with inhibition diameters of untreated *Bacillus* sp. CBEL-1 to check the alteration or loss in the resistance pattern [55].

3. Result and discussion

3.1. Characterization of photocatalyst

Metallic NPs usually have a strong surface Plasmon (SP) band in the UV-vis region due to the presence of free electrons on their surface. Coating their surface with a metal oxide layer is expected to change the dielectric constant of the environment immediate surrounding them and may shift (Red or Blue) their SP band. This concept has been employed to monitor the formation of first layer of metal oxide (SnO₂) shell on Ag NPs. As shown in Fig. 1(a), the bright yellow aqueous dispersion of Ag NPs has shown a clear and distinct SP band at 408 nm which has shifted to 435 nm after formation of SnO₂ shell on its surface. Similar observations were reported by Rai et al. [56] regarding the red shift of Ag NCs on formation of SnO₂ shell [56]. This was attributed to the increasing refractive index around the Ag NPs after formation of SnO₂ shell (SnO₂ refractive index is 2.0 which is much larger than that of water) [57]. On addition of sodium zincate (as a source of ZnO) on the colloidal dispersion of Ag@SnO₂, the color of the solution further changes to light brown and remarkable blue shift in the SP band to 411 nm were observed [32]. This suggests the formation of ZnO shell on Ag@SnO₂ NCs. It has been formerly reported that the SP bands are sensitive to chemical perturbations to the particle surface. ZnO with a refractive index of 1.92 is slightly less than that of SnO₂. Therefore, a blue-shift in the SP band was expected. Broadening of the SP band after double metal oxide shell coating, may have been resulted because of particle aggregation and clustering. Presence of a double shell, over the metallic core allows delayed e⁻-h⁺ recombination, due to the difference in their respective fermi levels [58]. Such systems could respond well as far as photocatalytic applications are concerned.

Phase and crystal configuration of Ag@SnO₂@ZnO NCs have been

investigated by XRD and shown in Fig. 1(b). For as synthesized NCs, three distinct peaks of Ag with $2\Theta = 44.321, 45.370$ and 64.814 corresponding to (200), (100) and (220) were observed (JCPDS Card No. 04-0783 and 41-1402). Ag NPs were expected to have a FCC structure. The XRD pattern also showed clear peaks at $2\Theta = 23.4077, 26.017, 27.796, 28.992, 38.737, 39.865, 46.304, 51.312, 52.349$, and 57.599 corresponding to (220), (110), (311), (222), (012), (101), (111), (211), (212) and (002) planes of for tin dioxide with a tetragonal structure (JCPDS card No. 33-1374, 21-1250, 03-1114, 29-1494). Peak corresponding to SnO_2 was observed with 2 theta value of 51.312 and 52.368 corresponding to plane value (211) and (212) was observed. Suggesting stable interaction between the inner core and the first shell (JCPDS card no. 44-1300). Similarly all the major peaks of ZnO with hexagonal wurtzite structure were observed at $2\Theta = 31.297, 33.756, 34.438, 36.685, 48.185$ and 55.240 which corresponds to (111), (202), (002), (101), (102) and (102) planes of ZnO respectively (JCPDS card no. 36-1451, 05-0664, 13-0311, 03-0888, 01-1136) [31–33,56,57]. Any peak corresponding to Sn-Zn and Ag-Zn was not observed suggesting that the materials retain their physical structures and suggesting the formation of NCs rather than the formation of any alloy [33,57].

To study the surface properties of the NCs, FTIR analysis was performed and result is shown in Fig. 1(c). The broad band existing between $3200\text{--}3600\text{ cm}^{-1}$ specifically at ($3325, 3396, 3460, 3600\text{ cm}^{-1}$) corresponds to vibrations from the O–H group, and the stretching vibrations at 2345 cm^{-1} resembles that of acidic O–H group. Small peaks appearing between 2900 to 3000 specifically at 2970 resembles the C–H group stretching mode. Moreover, the other small vibrations appearing at 1636 cm^{-1} belongs to the stretching from C=O group. Vibration peaks at 1521 cm^{-1} corresponds to C–H bending or from different hydroxyl hybrids which may have resulted from the synthesized oxides. The symmetric stretching at 1375 cm^{-1} indicates the vibration of NO_3^{-1} ions existed from the zinc nitrate used for core-shell synthesis of ZnO . The weak band of C–N group is observed at 1200 cm^{-1} . The peaks at 1636 cm^{-1} corresponds to Zn–O stretching as well, and 655 and 612 cm^{-1} may be a result of deformed vibrations [32,56,59].

Morphology of the $\text{Ag@SnO}_2@\text{ZnO}$ NCs was investigated by TEM and results are shown in Fig. 2(a–c). Near spherical morphology with core–shell structure of the NCs is clearly observed from these images. However, particles are obtained with multiple Ag@SnO_2 encapsulated inside the outer zinc oxide shell. The size of the as synthesized $\text{Ag@SnO}_2@\text{ZnO}$ NCs was in the range of $39\text{--}46\text{ nm}$. Metal core was found to have inter-planar spacing of $\sim 0.227\text{ nm}$ [Fig. 2(d)] which corresponds to the (111) plane of the metallic silver with FCC structure [32,33,56]. The Ag core was found to have a diameter of $10\text{--}12\text{ nm}$ with an outside uniform oxide shell of 16 to 18 nm thickness (This further involves two shells of SnO_2 and ZnO whose thickness are 10 nm and 6 nm respectively). TEM EDAX technique is used to understand the chemical composition of the as synthesized NCs. As shown in Fig. 2(e), $\text{Ag@SnO}_2@\text{ZnO}$ NCs have shown clear peaks corresponding to O, Sn, Zn, and Ag. Peaks corresponding to Cu and C are also obtained which may be a result of using carbon grid for depositing samples before TEM analysis [60].

3.2. Solar-SPCD of MDR *Bacillus* sp. CBEL-1

The time dependent SPCD potency of *Bacillus* sp. CBEL-1 was studied as per the reductions in the viable bacterial cell count. This is expressed in terms of ratio between N/N_0 where N corresponds to the viable cell count at a particular time point and N_0 corresponds to the initial bacterial load. Also the Log value was taken in accordance to study the Chick-Watson model for bacterial disinfection kinetics [61,62]. 500 mg/L of $\text{Ag@SnO}_2@\text{ZnO}$ NCs was found optimum for 5.1549 Log reduction of $1 \times 10^7\text{ CFU/mL}$ of targeted bacteria in 180 min and no viable bacteria were observed at 210 min suggesting complete disinfection as shown in Fig. 3(a) [and Supporting data Fig. S2(a)]. At 300 and 700 mg/L NCs concentrations, incomplete

disinfection was observed which could be due to inadequate ROS production and catalyst shielding effect respectively [44]. When the disinfection potency was assessed for the two experimental controls, PL also showed disinfection kinetics upto 5 Log reduction of the bacteria in 210 min [Fig. 3 (b) and Supporting data Fig. S2(b)]. Whereas the non-toxic properties of the NCs were confirmed by the DC results indicating only 0.03 bacterial Log reductions in 210 min . SPCD generates enough ROS within the system to be potent for the bacterial inactivation [24,44], whereas sunlight (PL treatment) since long has been reported as a potent inhibitor for a number of bacteria. The valid reasons could be certain membrane enzymes, photosensitizers and bio-molecules which upon irradiation with sunlight may shuttle or alter their free electrons to generate ROS within the membrane; this in turn may damage the membrane components of the bacteria to leave it compromised and untraceable to viable cell counting [63]. There have been reports suggesting intracellular generation of ROS inside bacterial cells due to Haber-Weiss reaction using intracellular iron and peroxide as initiator molecules [64]. From Fig. 3(c) [and Supporting data Fig. S2(c)], it is interesting to observe that, for every ten fold decrease in the initial bacterial load, the catalyst concentration required for complete disinfection was also reduced upto ten folds. Although the optimum catalyst concentration of 500 mg/L was suitable enough for complete disinfection of $1 \times 10^8\text{ CFU/mL}$ of target bacteria as the photocatalytic slurry system mostly needs the bacteria and catalyst in proper proportions for simultaneous generation of adequate ROS and avoid the catalyst shielding effect. The current data obtained can be attributed to this justification. From here onwards all the experiments were performed with initial bacterial count of $1 \times 10^7\text{ CFU/mL}$ and catalyst concentration of 500 mg/L [32,44,65]. India being a tropical country receives different intensity of sunlight throughout the year. The current study involves checking the SPCD potency of NCs under different sunlight intensities ranging between $50,000$ to $100,000\text{ lx}$. From the Fig. 3(d) [and Supporting data Fig. S2(d)], it is observed that, light intensity is indirectly proportional to the disinfection kinetics and time required for complete disinfection. Indian winters receive sunlight with nearly $45,000\text{--}50,000\text{ Lux}$ [66]. As per this study a minimum of $50,000 \pm 5000\text{ lx}$ is essential for complete killing of bacteria in 240 min . This supports to the fact that the present technology can be effective in winters with diffused sunlight [66]. In the present study, initially for 30 min the NCs and the target bacteria was kept incubated under stirring conditions to attain an equilibrium phase. Since the NCs used in the study are not toxic unless or until exposed to solar irradiation, it is quite expected that no or negligible disinfection or bacterial killing shall be occurring. This justification can be reconfirmed from the dark control data in Fig. 3(b), where even after the complete incubation time, the cell viability is maintained. Thus we are obtaining a shoulder phase. The initial disinfection time starts only after first 30 min of incubation. As we can clearly see that there is a sharp decrease in the N/N_0 value after 30 min , it is expected to follow Chick-Watson kinetics [Supporting data Fig. S2]. Similar results have also been observed for many of the previous reports [45,66].

It is well documented about the post disinfection reactivation of bacteria subjected to sunlight irradiation and SPCD. In the current study the post solar-SPCD reactivation of the target bacteria was studied till 96 h . From Fig. 4(a), no reactivation of the target bacteria in the solar-SPCD treated system was noticed till 96 h , unlike the PL and DC where substantial reactivation of the target bacteria was observed within 24 h post disinfection. This further proves the potency of SPCD for complete bacterial disinfection with no chances of triggering its damage repair machinery to reactivate [31]. This data has been validated in the later part of this study. When the SPCD experiments were validated with different photocatalysts, Ag@ZnO was found as superior as $\text{Ag@SnO}_2@\text{ZnO}$ NCs, where complete disinfection was observed in 210 min [Fig. 4(b)]. However, even after 210 min , no complete disinfection was observed in case of TiO_2 and ZnO NPs. The post SPCD reactivation studies confirmed no bacteria in case of Ag@ZnO unlike TiO_2 and ZnO .

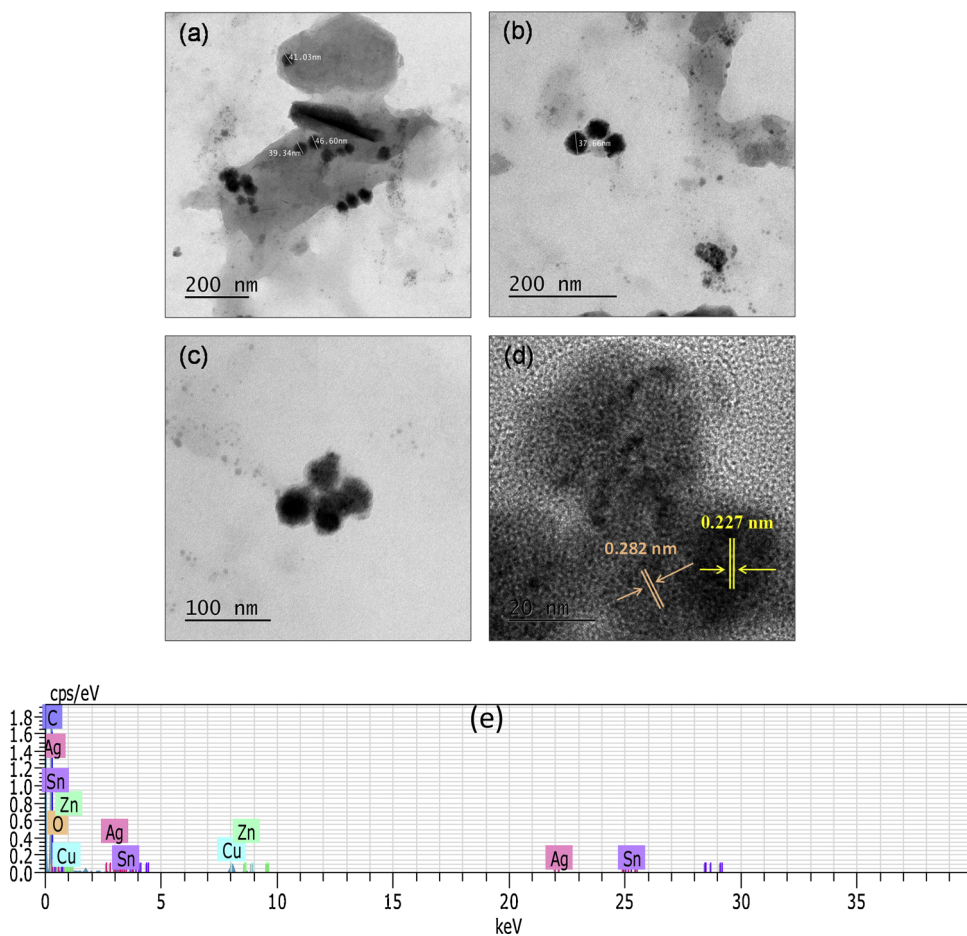


Fig. 2. TEM (a, b, and c) HRTEM (d) and EDAX (e) images of Ag@SnO₂@ZnO NCs.

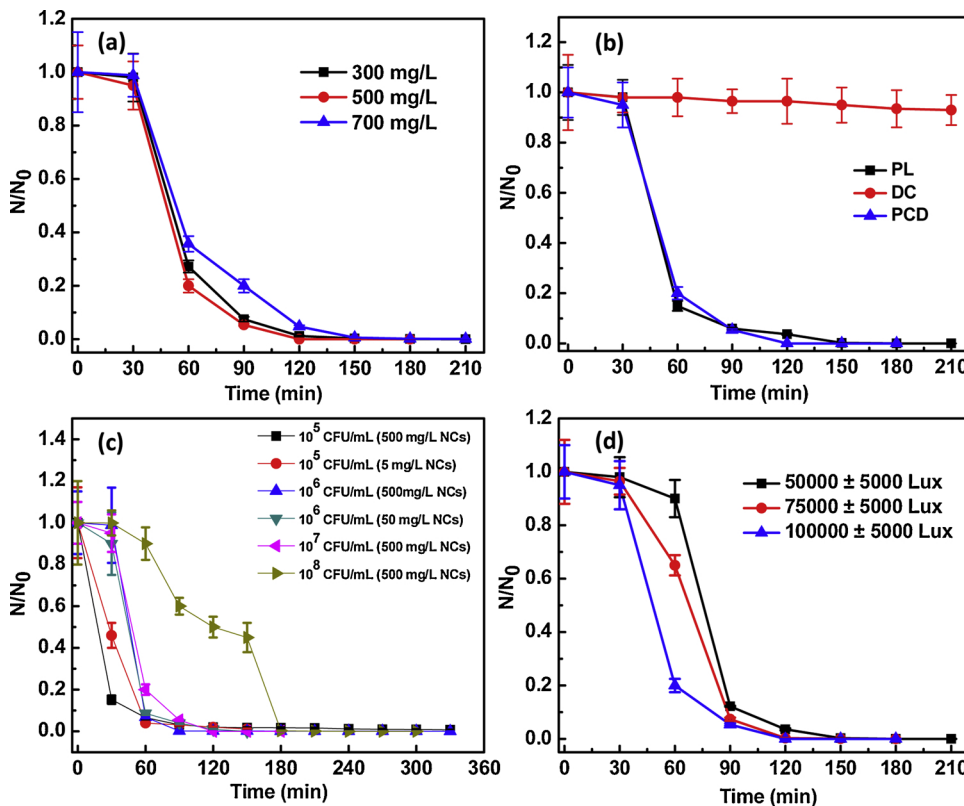
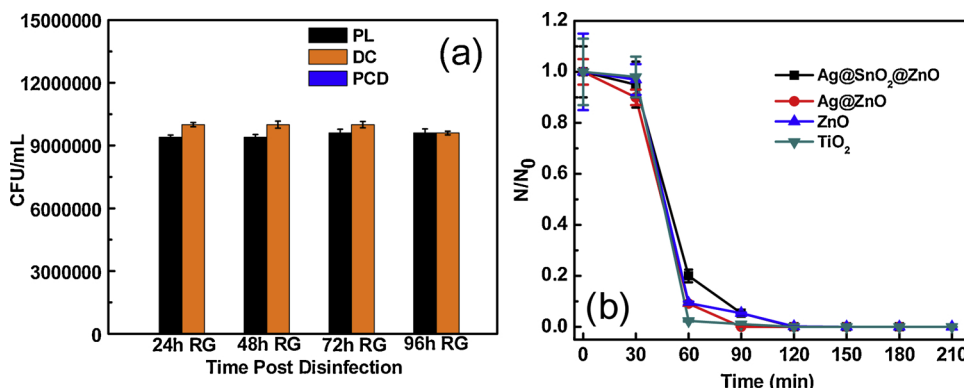


Fig. 3. (a) Effect of Ag@SnO₂@ZnO core-shell NC loading on the solar-PCD of *Bacillus* sp. CBEL-1, (b) Comparison of SPCD with PL and DC, (c) Effect of initial bacterial load on the solar-PCD of *Bacillus* sp. CBEL-1, (d) Effect of light intensity on the solar-PCD of *Bacillus* sp. CBEL-1. Initial bacterial concentration = 1×10^7 CFU/mL [Except in (c), where bacterial load is varied], [NCs or Ag@SnO₂@ZnO] = 500 mg/L [Except in (a) and (c) where NCs concentration is varied], Temperature = 35 ± 2 °C, pH = 6.8. Error bars indicate the standard deviation of replicates ($n = 3$).



Earlier studies from our group had reported the superiority of Ag@ZnO NCs for SPCD applications, where the efficiency of core-shell structure has been attributed to its structural stability and integrity in harsh environmental conditions. Interesting observations were made in case of all the traditional disinfectants, where within 30 min of treatment no viable bacteria were observed in NA plates (data not shown). However, substantial reactivation of the bacteria was observed after 24 h post reaction in case of all traditional disinfectants (data not shown). H₂O₂ and UV-250 nm treatment shows reactivation of the bacteria after 24 h but with reduced antibiotic resistance, this has been discussed in the later part of this study. The probable reasons to justify this could be, traditional disinfectants are always a faster means of combating pathogenic bacteria, but for longer exposure time, their efficacy restricts and gives enough time to the bacteria for triggering its damage repair machinery [67]. Moreover their action depends on the concentration and time of exposure. The robustness and resistance pattern of isolated bacteria heads responsible for its reactivation even after long term exposures [67,68].

3.3. Analysis of peroxidized membrane lipids of bacteria

As per the time dependent viable cell count data are concerned, the PL and SPCD both shows disinfection of *Bacillus* sp. CBEL-1. In both the cases the membranes were the primary targets from indirect and direct generation of ROS which subsequently leads to peroxidation of membrane lipids and generation of MDA. Fig. 5 (a) shows, at 60 min of treatment, maximum of 1.15 nmol and 0.9 nmol of MDA was quantified per mg cell dry weight for SPCD and PL respectively. Whereas MDA released was quite lesser in DC and untreated bacteria [44]. Peroxidized membrane lipids or oxidative stress has another biomarker called 4-HNE. Time dependent release of 4-HNE was studied using spectrophotometer to know the extent of oxidative stress. Fig. 5(b) shows SPCD treated bacteria has increased absorbance for 4-HNE at 200 nm up-to 210 min unlike the PL. DC shows comparatively lesser release of 4-HNE till 210 min. Thus release of both MDA and 4-HNE shows

Fig. 4. (a) Post-disinfection reactivation efficiency of *Bacillus* sp. CBEL-1 and (b) Effect of different photocatalysts on the solar-PCD the *Bacillus* sp. CBEL-1. Initial bacterial concentration = 1×10^7 CFU/mL, Temperature = 35 ± 2 °C, pH = 6.8, [Ag@SnO₂@ZnO] = 500 mg/L. Error bars indicate the standard deviation of replicates (n = 3).

compromization of the bacterial membrane. Moreover 4-HNE has been previously reported to hamper the intracellular protein and DNA content of the bacteria and may be responsible for phenotypic alterations in bacteria [46]. 4-HNE may react with cell based nucleophiles like thiols from glutathione and cysteine, amino group of lysine, imidazoles from histidine to undergo protein carbonylation and alterations [45]. It impairs the DNA damage repair machinery in bacteria and thus synergistically with the ROS induces irreversible damages to intracellular DNA and leaves no alternative for any repair as observed in this study [37,46].

3.4. Analysis of change in membrane fatty acid components of bacteria

Alteration in membrane fatty acid components justify the stress that the bacterial cell must have undergone. Omega-9 fatty acids contribute in tackling cardiovascular diseases caused by active stress [69,70]. Also we found an increase in fatty acids like cis-11 eicosenoic acid methyl ester (20:1 w9c) and cis-9 octadecanoic acid Methyl ester (18:1 w9c) after SPCD 180 min, which usually hikes because of oxidative stress (Supplementary Table-S2). The two aforesaid facts drive us towards pondering over omega-9 fatty acids that it has more tolerant and protective role towards oxidative stress or ROS. Moreover Omega 7 fatty acids like 20:1 w7c also may have immunomodulatory effects, thus their chances of getting increased during SPCD is quite relevant. The overall fluidity of the membrane remains compromised due to oxidative stress, hence the presence of such omega-9 and 7 fatty acids maintains overall membrane fluidity [69,71]. Octadecanoic acid (C18:0) was found to be increased after SPCD, which may be due to de-saturation under oxidative stress. All together these findings may conclude the highly oxidative environment that the NCs would have generated in the SPCD system. The bacteria in response possess change in their membrane lipid composition, which remains insufficient for its survival on further exposure time thus leaving their membrane completely damaged.

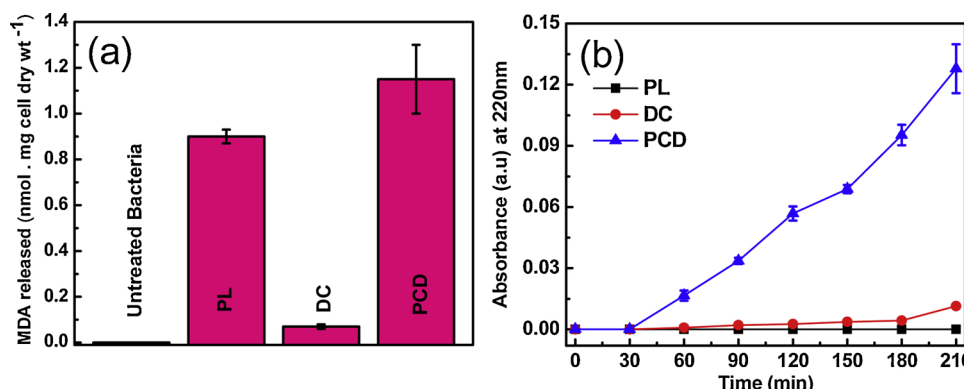


Fig. 5. Lipid peroxidation kinetics of *Bacillus* sp. CBEL-1: (a) MDA released after 60 min of SPCD treatment and (b) Time dependent release of 4-HNE in comparison to respective controls PL and DC. Initial bacterial concentration = 1×10^7 CFU/mL, Temperature = 35 ± 2 °C, pH = 6.8, [Ag@SnO₂@ZnO] = 500 mg/L. Error bars indicate the standard deviation of replicates (n = 3).

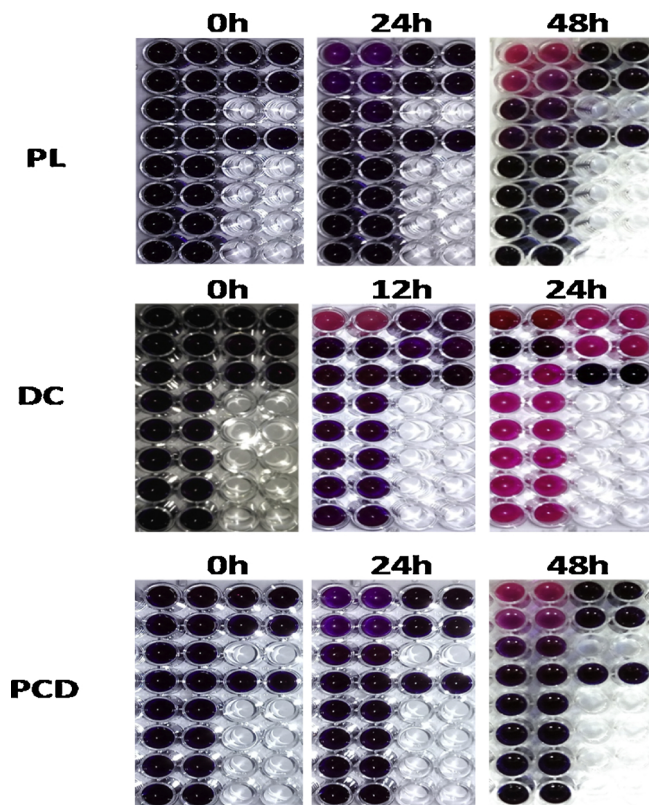


Fig. 6. Time dependent loss in metabolic activity of *Bacillus* sp. CBEL-1 after SPCD treatment along with controls, change in blue to pink confirms no metabolic damage (For interpretation of the references to colour in this figure legend, the reader is referred to the web version of this article).

3.5. Analysis of time dependent loss in metabolic activity of bacteria

The lipid peroxidation results were revalidated with loss in metabolic property of the bacterial electron transport system. From the resazurin assay, it was observed that after 90 and 60 min of treatment in PL and SPCD respectively, no blue to pink transformation of resazurin to resoforin was observed even after 48 h of incubation Fig. 6. This suggests complete loss in the membrane metabolic activity or more specifically the membrane oxidoreductase enzyme. However, most of the samples in DC turned pink within 12–24 h, indicating the non-interference of NCs with bacterial membrane oxidoreductase. Similar reasons could be attributed for this result as mentioned for viable cell count and membrane lipid peroxidation where most of the membrane damage is being caused by the direct and indirect generation of ROS. These ROS oxidizes the membrane enzymes and proteins thus altering the membrane metabolic potential of the target bacteria [37].

3.6. Time dependent release in cellular biomolecules and ions during SPCD

It has been reported in our previous study that, lipid peroxidation at greater extents can leave the membrane perturbed and thus making way for leakage of cellular biomolecules like DNA and protein into the reaction system. The time dependent increase in DNA and Protein was evident from Fig. 7(a) and (b). It has been found that after 60 min of solar-SPCD the DNA leakage has started and increased upto 11.4 µg/mL in 210 min. In PL and DC the DNA leakage was comparatively lesser which hiked upto 2.45 and 4.35 µg/mL in 210 min. The justified reasons for DNA leakage in the PL could be continuous mechanical shear stress due to agitation and intracellular damage and single stranded breaks in some amount of DNA by intracellular generation of photo-sensitizers mediated ROS [63]. Whereas in DC the hindrance caused by some NCs on the bacterial membrane, which leaves the bacterial DNA

find its way into the reaction slurry and subsequently detected in spectrophotometer. The protein leakage data of SPCD suggests increasing concentrations of protein into the system from 90 min onwards which hikes upto 180 µg/mL in 210 min, whereas at similar time point the protein leakage in PL and DC was negligible [37]. Thus leakage of cellular bio-molecules into the system suggests compromised bacteria due to simultaneous generation of ROS and 4-HNE thus adding more confirmation towards the photocatalytic damage to DNA and protein of bacteria [46].

3.7. Analysis of the bacterial cell membrane damage by Live/Dead staining

Results from fluorescence microscopy images from the live dead experiments are expected to give further confirmations about SPCD mediated killing of bacteria. Syto-9 Dye usually stains live bacteria and its cytoplasm, whereas PI stains dead bacteria in its nucleic acids [72]. From Fig. 8, it is evident that till 210 min of PL [Fig. 9 (a to e)] and DC treatment [Fig. 8 (f to j)], there is no transformation of bacteria from green to red color. It suggested slight or no impermeability to bacterial membrane which would have allowed the PI to enter and stain the bacterial DNA red. Distinct color change from green to red was observed in SPCD treated sample from 90 min onwards, which intensifies upto 210 min living behind no clue of green color acquired live bacteria, due to substantial membrane damages [Fig. 8 (k-o)]. These results correspond well with our post disinfection reactivation studies, where extensive reactivation of bacteria was found in PL and DC treated sample [31]. Sunlight only (PL) may have induced temporary inactivation of the bacteria, which trigger its damage repair machinery into action once put back in dark for 24 h. This was unlike SPCD where the photocatalytic damage was quite enduring as evident from the PI (red) stained bacteria, allowing no bacterial reactivation [31].

3.8. Analysis of bacterial membrane damage by electron microscopy

The results obtained from live/Dead assay were further confirmed from FESEM analysis of the SPCD treated bacteria and its respective controls. Fig. 9 shows stepwise loss in structural integrity of bacteria after 120 and 210 min SPCD Fig. 9 (e and f) respectively, where the bacteria have completely transformed into cellular debris. No such change was observed in case of PL and DC treated bacteria, where the structural integrity of the bacteria was well maintained even after 210 min of treatment [Fig. 9 (c and d)]. Fig. 9 (e) shows the compromised bacteria after 120 min SPCD, perhaps around this time point, the bacterial membrane is fully impaired and most of the intracellular biomolecules get leaked into the system [37,73].

3.9. Detection of primary reactive oxygen species involved for SPCD

It has been established with different set of experiments that NCs used in the current SPCD study is quite efficient for irreversible disinfection of *Bacillus* sp. CBEL-1. This further necessitates to track the major ROS out of H_2O_2 , O_2^- , OH^- , h^+ , and e^- involved for disinfection of the targeted bacteria. As shown in Fig. 10, when scavengers for individual ROS were added in the system it was found that at 180 min of treatment, the bacterial disinfection or Log reductions in presence of Fe-EDTA (For H_2O_2) and Tempol (O_2^-) and Sodium oxalate (For h^+) were minimal i.e. around 3.52, 3.72 and 4.22 respectively. Whereas in the scavenger less condition, the Log reduction was 5.15. Interesting observations were made after addition of Cr(VI) (scavenger for e^-) and Isopropanol (scavenger for OH^-), where their addition into the system intensifies the disinfection kinetics to 6 and 7 Log reductions respectively. The antimicrobial actions of both Cr(VI) (potassium dichromate) and isopropanol have been long reported in various literatures, the present increase in disinfection kinetics could be attributed to these aforementioned reason. Suggesting H_2O_2 and O_2^- being active ROS generating in the system and killing of the bacteria *Bacillus* sp. CBEL-1

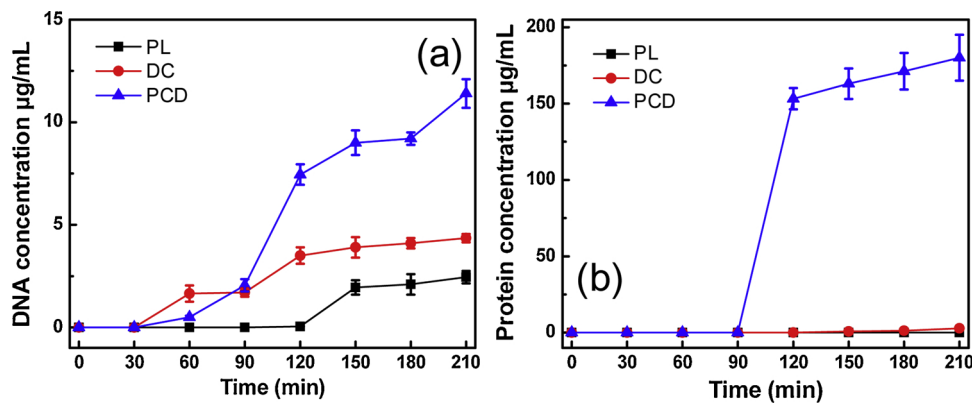


Fig. 7. Time dependent leakage of (a) DNA and (b) protein after SPCD in comparison to respective controls. Initial bacterial concentration = 1×10^7 CFU/mL, Temperature = 35 ± 2 °C, pH = 6.8, $[\text{Ag@SnO}_2@\text{ZnO}] = 500$ mg/L. Error bars indicate the standard deviation of replicates ($n = 3$).

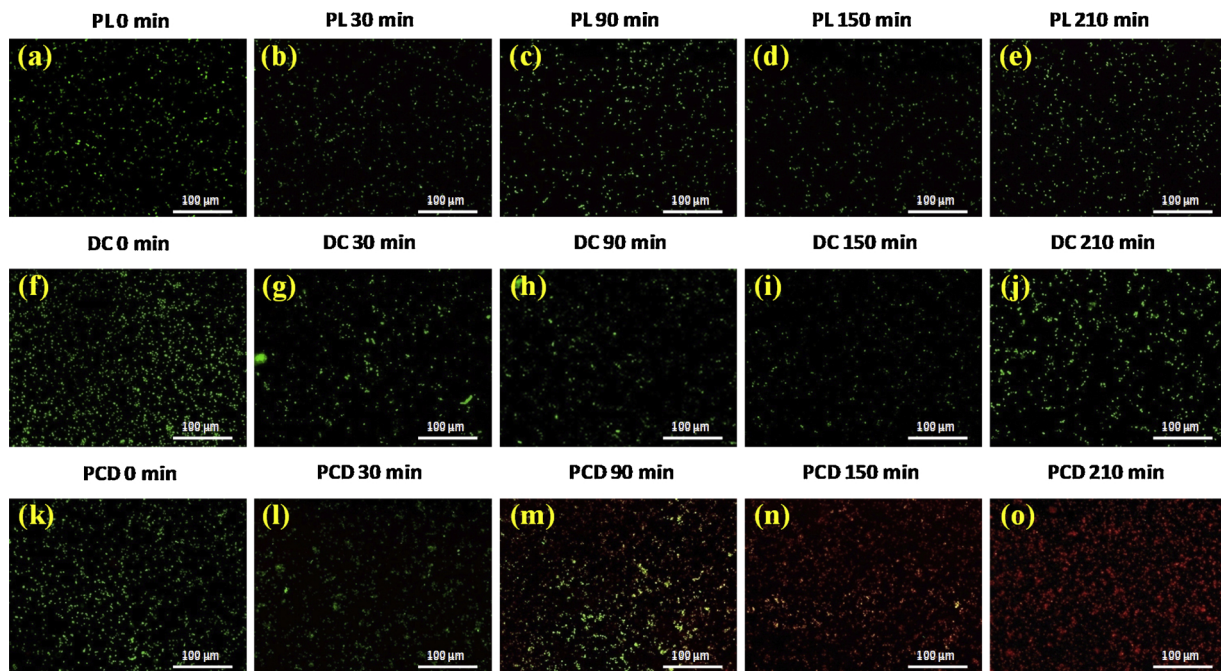


Fig. 8. (a) to (e) shows the fluorescent microscopic images of light control treatment of *Bacillus* sp. CBEL-1 without the presence of catalyst at 0, 30, 90, 150 and 210 min respectively. (f) to (j) shows fluorescent microscopic images of dark control treatment of *Bacillus* sp. CBEL-1 without the presence of light at 0, 30, 90, 150 and 210 min respectively (with $[\text{Ag@SnO}_2@\text{ZnO}] = 500$ mg/L). (k) to (o) shows the fluorescent microscopic images of *Bacillus* sp. CBEL-1 that was subjected to SPCD in presence of $\text{Ag@SnO}_2@\text{ZnO}$ NCs ($[\text{Ag@SnO}_2@\text{ZnO}] = 500$ mg/L) at 0, 30, 90, 150 and 210 min respectively.

[41]. The findings from this result were relative to our previously reported SPCD of MDR *E. coli* using Fe-doped ZnO [31].

3.10. Stability of the photocatalyst

The crystal structure of the photocatalyst could be amended by the chemical species present in the reaction slurry which in turn may alter the photocatalytic activity. This has been one of the serious challenges of SPCD for real world application. Therefore stability of the $\text{Ag@SnO}_2@\text{ZnO}$ NCs in post reaction condition was investigated using XRD and no change in crystal structure of material was observed [32]. This indicates its structural stability throughout the process. A slight decrease in the intensity of the XRD peaks was noticed which could be due to loss of materials during sample washing and recovery (Data not shown). There has been a concern about leaching of metal ions in the treated water which could re-toxify the system. It could also be proclaimed that Ag^+ , Sn^{2+} and Zn^{2+} ions which are known to have antimicrobial property may leach out of the system and hence, may be the

reason behind disinfection process. To further eradicate this possibility, water sample subjected to SPCD was analyzed by atomic absorption spectroscopy (AAS, Agilent Technologies Inc.) to detect the presence of metal ions [31,38]. Detectable amount of Ag^+ , Sn^{2+} and Zn^{2+} ions were not obtained.

3.11. Investigation of efficiency of solar-SPCD in real water samples

Disinfection of *Bacillus* sp. in real water systems has been done to check the applicability of NCs based photocatalysis for real world applications. Complete disinfection of the target bacteria, was noticed in 150 to 210 min for all the real water systems as shown in Fig. 11. Lake water was found to have a pH of 6.21 (Data Given in Supplementary Table-S3) which is slightly on the acidic side, hence we can infer that acidic pH may negatively influence the disinfection process, but ultimately lead to the complete disinfection of the microorganisms without any reactivation [31]. Conductivity, salinity and total dissolved solids were found to have negligible influence on the SPCD process, as

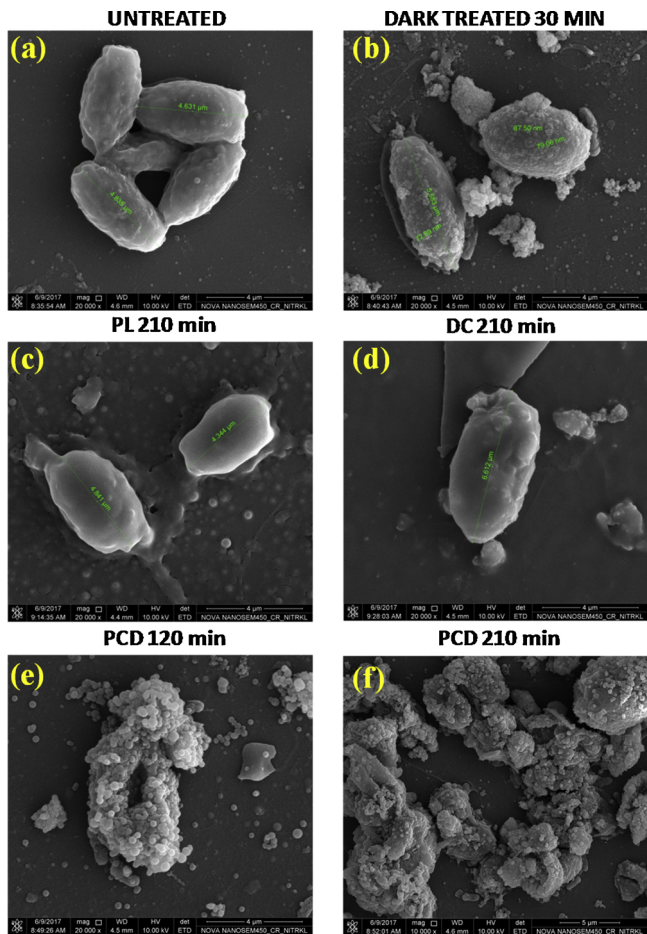


Fig. 9. (a) and (b) shows the FESEM images of the untreated bacteria and dark control (in the absence of light and treated with $[Ag@SnO_2@ZnO] = 500 \text{ mg/L}$ for 30 min), PL 210 min (c), DC 210 min (d), SPCD 120 min and 210 min (e and f).

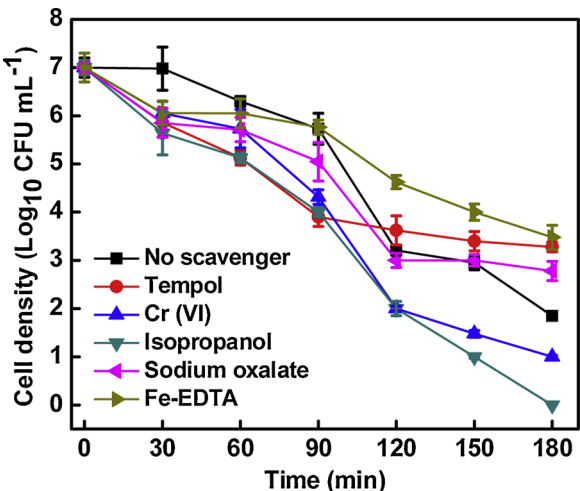


Fig. 10. Effect of different scavengers on the SPCD of *Bacillus* sp. CBEL-1 in presence of $Ag@SnO_2@ZnO$ NCs. Initial bacterial concentration = $1 \times 10^7 \text{ CFU/mL}$, Temperature = $35 \pm 2^\circ\text{C}$, pH = 6.8, $[Ag@SnO_2@ZnO] = 500 \text{ mg/L}$. Error bars indicate the standard deviation of replicates ($n = 3$).

complete disinfection of the target bacteria was observed in all the water samples. The treated bacteria spiked real water were kept for 7 days post disinfection to find no clue of bacterial reactivation from viable cell count analysis. Such effective disinfection kinetics under the

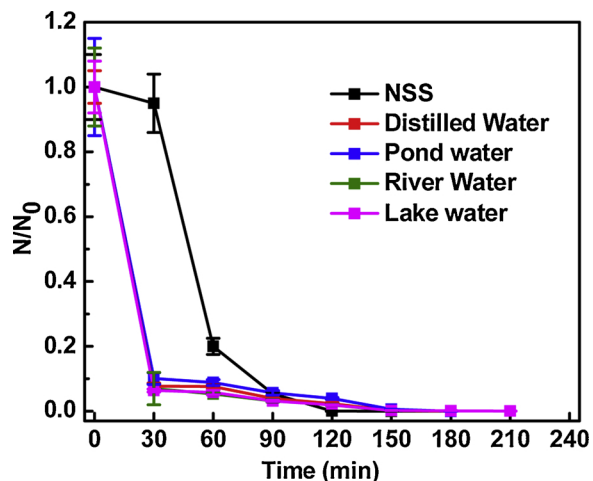


Fig. 11. Effect of $Ag@SnO_2@ZnO$ on the relative reduction in the *Bacillus* sp. CBEL-1 cell count (N/N_0) in real water samples after 210 min of solar irradiation at a catalyst loading of 500 mg/L.

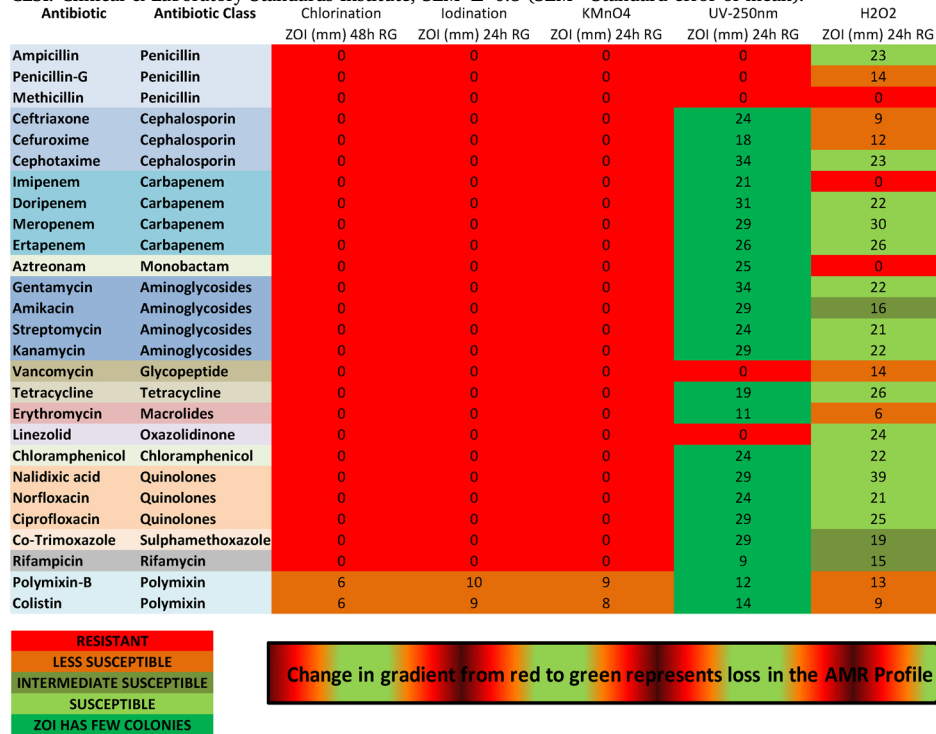
influence of pH in between 6–8, conductivity upto 153 mS/cm, total dissolved solids upto 115 ppm and salinity of 133 ppm lays the foundation for NCs mediated photocatalysis to be used against MDR microorganisms in real water matrices for sustainable environment and public health [31].

3.12. Assessing the antibiotic resistance pattern after disinfection

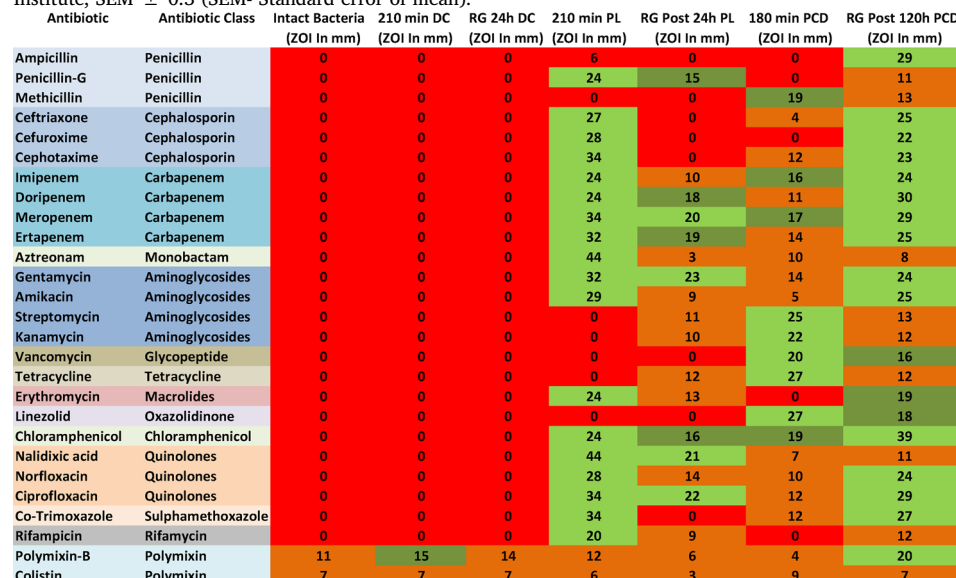
Although traditional disinfection techniques like chlorination ($NaOCl$), iodination (KI), treatment with potassium permanganate ($KMnO_4$), UV Light (250 nm) and hydrogen peroxide (H_2O_2) have been used since long disinfection of contaminated water, their implication drastically failed in this case for successful and complete disinfection of *Bacillus* sp. CBEL-1. Though in each of this treatment as mentioned earlier no viable cell count were obtained after 30 min of treatment, but substantial reactivation of the bacteria was observed 24 h post disinfection. The disinfection performance was better in H_2O_2 were the reactivated bacteria was observed to have some loss in their antibiotic resistance profile as shown in Table 1 [55]. The data from the UV treatment was also convincing until it was found that the 24 h reactivated culture has mixed colonies with and without loss of antibiotic resistance [Table 1]. The data for change in antibiotic resistance of the bacteria after different traditional disinfection treatment have been shown in the Table 1 [74]. The change in antibiotic resistance pattern of *Bacillus* sp. CBEL-1 after SPCD and its respective controls were performed. From the Table 2 it was observed that 180 min of SPCD treatment leads to the loss in resistance to carbapenem, aminoglycosides, monobactam, glycopeptide, tetracycline, oxazolidone, chloramphenicol, quinolones and sulphamethoxazole. Interesting observation were made, where 1 colony was found to be re-grown after 120 h of post SPCD was found susceptible to all the groups of antibiotics and with complete loss of resistance. In case of control experiments, PL 210 min leads to the loss in resistance for penicillin-G, cephalosporins, carbapenem, monobactam, aminoglycosides (except streptomycin and kanamycin), macrolides, chloramphenicol, quinolones, sulphamethoxazole and rifamycin. Interesting observations were found in the resistance pattern of PL treated bacteria after 24 h RG, where the bacteria acquired back its resistance to cephalosporins, sulphamethoxazole and a bit to rifamycin, quinolones, chloramphenicol, macrolides, monobactam and carbapenem, as per the ZOI data. This suggests that PL could lead to inhibition of bacteria, but when incubated in dark post disinfection could revert back its resistance profile [75]. DC does not lead to loss of the resistance for nearly all the antibiotic groups neither after 210 min of treatment nor 24 h post treatment RG [55].

Table 1

Schematic representation showing change in antibiotic resistance profile of *Bacillus* sp. CBEL-1 subjected to different traditional chemical disinfection treatments after post disinfection reactivation. * ZOI = Total zone (including the disc) – Diameter of the disc (6 mm). Red-Resistant Green-Susceptible, Experiments performed as per CLSI: Clinical & Laboratory Standards Institute, SEM \pm 0.3 (SEM—Standard error of mean).

**Table 2**

Schematic representation showing change in antibiotic resistance profile of *Bacillus* sp. CBEL-1 subjected to SPCD, PL and DC and after post disinfection reactivation. * ZOI = Total zone (including the disc) – Diameter of the disc (6 mm). Red-Resistant Green-Susceptible, Experiments performed as per CLSI: Clinical & Laboratory Standards Institute, SEM \pm 0.3 (SEM- Standard error of mean).



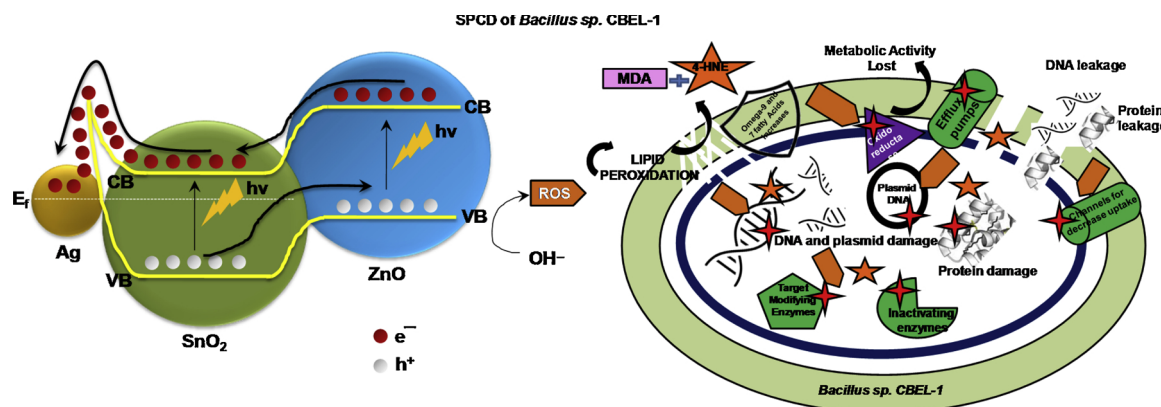


Fig. 12. Schematic view of solar-PCD of *Bacillus* sp. CBEL-1 in presence of Ag@SnO₂@ZnO NCs.

From the Table 2 it can be inferred that, both PL and SPCD are efficient for changing the AMR profile of the *Bacillus* sp. CBEL-1. It is quite interesting to notice that, with PL treatment, the bacteria reactivates within 24 h post disinfection and is gaining back the resistance again unlike the SPCD treatment. In SPCD the effect of disinfection was more prominent and disallowing the bacterial re-growth till 96 h post disinfection [31]. At 120 h post disinfection, 1 colony was observed in the agar plate and was found sensitive to all the antibiotics used in this study as per the ZOI data. Thus it can be inferred that though the bacteria reactivates after 120 h, but its corresponding resistance is completely lost. AOP or SPCD treatment thus may be hampering the various ways by which the bacteria acquire resistance to different antibiotics. Possibly the ROS in the system could be damaging various efflux pumps and drug channels, different drug inactivating enzymes, target modifying enzymes and more specifically the genetic content of the bacterium rendering them sensitive to antibiotics [76]. It can be inferred that, ZnO based photocatalysts are more efficient as compared to TiO₂ based systems for disinfection of the MDR *Bacillus* sp. CBEL-1 and subsequent loss of antibiotic resistance (Supplementary Table-S4). Ag@ZnO and Ag@SnO₂@ZnO were found much effective for loss in antibiotic resistance of *Bacillus* sp. CBEL-1 after SPCD as compared to ZnO, but Ag@SnO₂@ZnO possessing advantages in terms of ease of synthesis, better NCs yield and post SPCD reaction separability and reusability have been chosen for further experiments.

3.13. Proposed disinfection mechanism

Based upon the experimental observations a simple disinfection mechanism is proposed (Fig. 12). Conventionally, when light of suitable wavelength is irradiated on the semiconductor NPs (e.g. ZnO or SnO₂), electron (e⁻) and hole (h⁺) separation is realized. However, in case of pure semiconductors, e⁻ / h⁺ are expected to undergo a fast recombination process which makes them unavailable for photocatalytic application. However, in the present case formation of a SnO₂/ZnO heterojunction is expected. Under this condition, their different work functions facilitates the movement of negatively charged carriers from SnO₂ (the material with low work function) to ZnO (the one with high work function) until their Fermi levels alignment is established (i.e., the system reaches the state of thermal equilibrium), which leads to the creation of an electrostatic field at the interface. At thermal equilibrium, the conduction band (CB) and valence band (VB) of SnO₂ and ZnO tends to bend, and a depletion layer is formed around the interface. When the SnO₂/ZnO heterojunction is irradiated by sun-light with photon energy higher or equal to the band gaps of SnO₂ and ZnO, e⁻ in the VB can be excited to the CB with simultaneous generation of the same amount of h⁺ in the VB [77]. The photogenerated e⁻ and h⁺ are separated under the influence of the electrostatic field induced by different work functions. Therefore, e⁻ move to the SnO₂ side of the

interface and h⁺ to the ZnO side. Additionally, photogenerated e⁻ can migrate from CB in SnO₂ to the surface of Ag NPs via Ag/SnO₂ interface further delaying e⁻ / h⁺ recombination process [78]. Synergistic role of these two phenomena could have increased the availability of h⁺ in the reaction system, thus helping in production of more ROS in case of Ag@SnO₂@ZnO mediated SPCD process. This high concentration of ROS is expected to have contributed not only to the killing of the MDR *Bacillus* sp. CBEL-1 but also may have hindered the re-growth of the bacteria after disinfection.

4. Conclusion

When a MDR *Bacillus* sp. CBEL-1 was subjected to Ag@SnO₂@ZnO NCs mediated SPCD, complete disinfection of the targeted pathogen was achieved within 210 min with a catalyst concentration of 500 mg/L without any further reactivation for 96 h post disinfection. The disinfection profile was validated using C-W disinfection model. Our investigations confirmed the involvement of H₂O₂ as the key ROS involved behind S of MDR *Bacillus* sp. CBEL-1. The post SPCD irreversible change in antibiotic resistance profile of the target bacteria was performed and substantial loss in the resistance was seen without recovery even after 96 h post disinfection. The effectiveness of disinfection was compared with traditional chemical disinfectants and UV-250 nm and found to have lesser impact on the resistance profile of the bacteria. Quantitative analyses of biomolecules and MDA released into the system proposed the damage of bacterial cell wall during SPCD. For the first time, increase in production of 4-HNE during PCD was reported along with change in fatty acid profile of bacteria after oxidative stress. Studying the irreversible effect of SPCD on morphology and structural integrity of the bacteria was confirmed by fluorescence microscopy and FESEM analysis. It was suggested that the targeted pathogen could not re-grow by using its DNA-repair mechanism as confirmed from re-growth and FESEM analysis. Disinfection achieved using the Ag@SnO₂@ZnO NCs were also validated for real world water samples from lake, pond and river. The developed photocatalytic process may be useful in designing an efficient and low cost water decontamination system to control enteric microbial pathogens including MDRs and hence may be useful to reduce spread of antibiotic resistance. This might reduce the risk of cholera and other diarrheagenic diseases and could be beneficial for improving the quality of life in both urban and economically backward rural areas. Current technology may be translated for on field application in the form of a device with proper validation using real hospital and municipal wastewater system for removal of MDRs and other water borne bacteria.

Declaration of Competing Interest

The authors declare that they have no known competing financial

interests or personal relationships that could have appeared to influence the work reported in this paper.

Acknowledgement

This work is supported by Department of Science and Technology, Government of India (Grant No. IFA12-ENG-37). This work is also partly supported by Swedish Research Council, Government of Sweden (Grant Nos. 2012-02889 and 2017-01327). Sourav Das is grateful to Council of Scientific and Industrial Research (CSIR), Government of India for supporting him by CSIR-Senior Research Fellowship programme [QS/1035(0009)/2016-EMR-I].

Appendix A. Supplementary data

Supplementary material related to this article can be found, in the online version, at doi:<https://doi.org/10.1016/j.apcatb.2019.118065>.

References

- [1] M.M. Mekonnen, A.Y. Hoekstra, Four billion people facing severe water scarcity, *Sci. Adv.* 2 (2016) e1500323.
- [2] A. Kuberan, A.K. Singh, J.B. Kasav, S. Prasad, K.M. Surapaneni, V. Upadhyay, A. Joshi, Water and sanitation hygiene knowledge, attitude, and practices among household members living in rural setting of India, *J. Nat. Sci. Biol. Med.* 6 (2015) S69.
- [3] W.H.O., W.U.J.W. Supply, S.M. Programme, Progress on Sanitation and Drinking Water: 2015 Update and MDG Assessment, World Health Organization, 2015.
- [4] W.H.O., 2.1 Billion People Lack Safe Drinking Water at Home, More Than Twice as Many Lack Safe Sanitation, 22 (2017) 2017.
- [5] A.M. Gall, B.J. Mariñas, Y. Lu, J.L. Shisler, Waterborne viruses: a barrier to safe drinking water, *PLoS Pathog.* 11 (2015) e1004867.
- [6] J. Brown, S. Cairncross, J.H. Ensink, Water, sanitation, hygiene and enteric infections in children, *Arch. Dis. Child.* 98 (2013) 629–634.
- [7] G. Sheeba, A. Jalagam, P. Venkatasubramanian, Drinking water contamination from peri-urban Bengaluru, India, *Curr. Sci.* 113 (2017) 1702.
- [8] F.A. Drobniowski, *Bacillus cereus* and related species, *Clin. Microbiol. Rev.* 6 (1993) 324–338.
- [9] C.U. Tuazon, H.W. Murray, C. Levy, M.N. Solny, J.A. Curtin, J.N. Sheagren, Serious infections from *Bacillus* sp., *JAMA* 241 (1979) 1137–1140.
- [10] N. Ramarao, L. Belotti, S. Deboscker, M. Ennahar-Vuillemin, J. De Launay, T. Lavigne, C. Koebel, B. Escande, M.H. Guinebretière, Two unrelated episodes of *Bacillus cereus* bacteraemia in a neonatal intensive care unit, *Am. J. Infect. Control* 42 (2014) 694–695.
- [11] G. Schaefer, W. Campbell, J. Jenks, C. Beesley, T. Katsivas, A. Hoffmaster, S.R. Mehta, S. Reed, Persistent *Bacillus cereus* bacteremia in 3 persons who inject drugs, San Diego, California, USA, *Emerging Infect. Dis.* 22 (2016) 1621.
- [12] F.A. Waldvogel, A.L. Bismo, Infections Associated with Indwelling Medical Devices, ASM Press, Washington, DC, 2000.
- [13] L.P. Stenf Arnesen, A. Fagerlund, P.E. Granum, From soil to gut: *Bacillus cereus* and its food poisoning toxins, *FEMS Microbiol. Rev.* 32 (2008) 579–606.
- [14] W.L. Nicholson, N. Munakata, G. Horneck, H.J. Melosh, P. Setlow, Resistance of *Bacillus* endospores to extreme terrestrial and extraterrestrial environments, *Microbiol. Mol. Biol. Rev.* 64 (2000) 548–572.
- [15] E. Reilman, R.A. Mars, J.M. van Dijken, E.L. Denham, The multidrug ABC transporter BmrC/BmrD of *Bacillus subtilis* is regulated via a ribosome-mediated transcriptional attenuation mechanism, *Nucleic Acids Res.* 42 (2014) 11393–11407.
- [16] A. Athamma, M. Athamma, N. Abu-Rashed, B. Medlej, D. Bast, E. Rubinstein, Selection of *Bacillus* anthracis isolates resistant to antibiotics, *J. Antimicrob. Chemother.* 54 (2004) 424–428.
- [17] E.Y. Klein, T.P. Van Boeckel, E.M. Martinez, S. Pant, S. Gandra, S.A. Levin, H. Goossens, R. Laxminarayan, Global increase and geographic convergence in antibiotic consumption between 2000 and 2015, *Proc. Natl. Acad. Sci. U. S. A.* 115 (2018) E3463–E3470.
- [18] J.M. Blair, M.A. Webber, A.J. Baylay, D.O. Ogbolu, L.J. Piddock, Molecular mechanisms of antibiotic resistance, *Nat. Rev. Microbiol.* 13 (2015) 42.
- [19] C.J. von Wintersdorff, J. Penders, J.M. van Niekerk, N.D. Mills, S. Majumder, L.B. van Alphen, P.H. Savelkoul, P.F. Wolfs, Dissemination of antimicrobial resistance in microbial ecosystems through horizontal gene transfer, *Front. Microbiol.* 7 (2016) 173.
- [20] M. Ferri, E. Ranucci, P. Romagnoli, V. Giaccone, Antimicrobial resistance: a global emerging threat to public health systems, *Crit. Rev. Food Sci. Nutr.* 57 (2017) 2857–2876.
- [21] W.H. Organization, Antimicrobial Resistance: Global Report on Surveillance, World Health Organization, 2014.
- [22] F. Baraneshme, M. Munir, Strategies to combat antibiotic resistance in the wastewater treatment plants, *Front. Microbiol.* 8 (2018) 2603.
- [23] J. Lu, T. Zhang, J. Ma, Z. Chen, Evaluation of disinfection by-products formation during chlorination and chloramination of dissolved natural organic matter fractions isolated from a filtered river water, *J. Hazard. Mater.* 162 (2009) 140–145.
- [24] M.N. Chong, B. Jin, C.W. Chow, C. Saint, Recent developments in photocatalytic water treatment technology: a review, *Water Res.* 44 (2010) 2997–3027.
- [25] O.K. Dalrymple, E. Stefanakos, M.A. Trotz, D.Y. Goswami, A review of the mechanisms and modeling of photocatalytic disinfection, *Appl. Catal. B* 98 (2010) 27–38.
- [26] T. Matsunaga, R. Tomoda, T. Nakajima, H. Wake, Photoelectrochemical sterilization of microbial cells by semiconductor powders, *FEMS Microbiol. Lett.* 29 (1985) 211–214.
- [27] P. Fernández-Ibáñez, M. Polo-López, S. Malato, S. Wadhwa, J. Hamilton, P. Dunlop, R. D'sa, E. Magee, K. O'shea, D. Dionysiou, Solar photocatalytic disinfection of water using titanium dioxide graphene composites, *Chem. Eng. J.* 261 (2015) 36–44.
- [28] Y. Jia, S. Zhan, S. Ma, Q. Zhou, Fabrication of TiO₂-Bi₂WO₆ binanosheet for enhanced solar photocatalytic disinfection of *E. coli*: insights on the mechanism, *ACS Appl. Mater. Interfaces* 8 (2016) 6841–6851.
- [29] D. Venieri, A. Fragedaki, M. Kostadima, E. Chatzisymeon, V. Binias, A. Zachopoulos, G. Kiriakidis, D. Mantzavinos, Solar light and metal-doped TiO₂ to eliminate water-transmitted bacterial pathogens: photocatalyst characterization and disinfection performance, *Appl. Catal. B* 154 (2014) 93–101.
- [30] J. Mac Mahon, S.C. Pillai, J.M. Kelly, L.W. Gill, Solar photocatalytic disinfection of *E. coli* and bacteriophages MS2, ΦX174 and PR772 using TiO₂, ZnO and ruthenium based complexes in a continuous flow system, *J. Photochem. Photobiol. B: Biol.* 170 (2017) 79–90.
- [31] S. Das, S. Sinha, B. Das, R. Jayabalan, M. Suar, A. Mishra, A.J. Tamhankar, C.S. Lundborg, S.K. Tripathy, Disinfection of multidrug resistant *Escherichia coli* by solar-photocatalysis using Fe-doped ZnO nanoparticles, *Sci. Rep.* 7 (2017) 104.
- [32] S. Das, S. Sinha, M. Suar, S.-I. Yun, A. Mishra, S.K. Tripathy, Solar-photocatalytic disinfection of *Vibrio cholerae* by using Ag@ZnO core-shell structure nanocomposites, *J. Photochem. Photobiol. B: Biol.* 142 (2015) 68–76.
- [33] G. Oldfield, T. Ung, P. Mulvaney, Au@SnO₂ core-shell nanocapacitors, *Adv. Mater.* 12 (20) (2000) 1519–1522.
- [34] L. Rizzo, A. Della Sala, A. Fiorentino, G.L. Puma, Disinfection of urban wastewater by solar driven and UV lamp-TiO₂ photocatalysis: effect on a multi drug resistant *Escherichia coli* strain, *Water Res.* 53 (2014) 145–152.
- [35] C.S. Lundborg, V. Diwan, A. Pathak, M.R. Purohit, H. Shah, M. Sharma, V.K. Mahadik, A.J. Tamhankar, Protocol: a 'One health' two year follow-up, mixed methods study on antibiotic resistance, focusing children under 5 and their environment in rural India, *BMC Public Health* 15 (2015) 1321.
- [36] F.R. Cockerill, Clinical, L.S. Institute, Performance Standards for Antimicrobial Susceptibility Testing: Twenty-third Informational Supplement;... Provides Updated Tables for... M02-A11, M07-A9, and M11-A8], National Committee for Clinical Laboratory Standards, 2013.
- [37] A.H. Rahman, A.J. Misra, S. Das, R. Jayabalan, M. Suar, A. Mishra, A.J. Tamhankar, C.S. Lundborg, S.K. Tripathy, Mechanistic insight into the disinfection of *Salmonella* sp. by sun-light assisted sonophotocatalysis using doped ZnO nanoparticles, *Chem. Eng. J.* 336 (2018) 476–488.
- [38] S. Das, N. Ranjana, A.J. Misra, M. Suar, A.J. Tamhankar, C.S. Lundborg, S.K. Tripathy, Disinfection of the water borne pathogens *Escherichia coli* and *Staphylococcus aureus* by solar photocatalysis using Sonochemically Synthesized Reusable Ag@ ZnO Core-Shell Nanoparticles, *Int. J. Environ. Res. Public Health* 14 (2017) 747.
- [39] E. Veschetti, D. Cutilli, L. Bonadonna, R. Briancesco, C. Martini, G. Cecchini, P. Anastasi, M. Ottaviani, Pilot-plant comparative study of peracetic acid and sodium hypochlorite wastewater disinfection, *Water Res.* 37 (2003) 78–94.
- [40] H. Backer, J. Hollowell, Use of iodine for water disinfection: iodine toxicity and maximum recommended dose, *Environ. Health Perspect.* 108 (2000) 679–684.
- [41] E. Linley, S.P. Denyer, G. McDonnell, C. Simons, J.-Y. Maillard, Use of hydrogen peroxide as a biocide: new consideration of its mechanisms of biocidal action, *J. Antimicrob. Chemother.* 67 (2012) 1589–1596.
- [42] T. Dai, M.S. Vrahas, C.K. Murray, M.R. Hamblin, Ultraviolet C irradiation: an alternative antimicrobial approach to localized infections? *Expert Rev. Anti. Ther.* 10 (2012) 185–195.
- [43] J. Cleasby, E. Baumann, C. Black, Effectiveness of potassium permanganate for disinfection, *J. Am. Water Works Assoc.* 56 (1964) 466–474.
- [44] P.-C. Maness, S. Smolinski, D.M. Blazek, Z. Huang, E.J. Wolfrum, W.A. Jacoby, Bactericidal activity of photocatalytic TiO₂ reaction: toward an understanding of its killing mechanism, *Appl. Environ. Microbiol.* 65 (1999) 4094–4098.
- [45] P.F. Stanbury, A. Whitaker, S.J. Hall, Principles of Fermentation Technology, 2nd ed, Elsevier, 1995.
- [46] H. Esterbauer, R.J. Schaur, H. Zollner, Chemistry and biochemistry of 4-hydroxynonenal, malonaldehyde and related aldehydes, *Free Radic. Biol. Med.* 11 (1991) 81–128.
- [47] M. Sasser, Bacterial Identification by Gas Chromatographic Analysis of Fatty Acids Methyl Esters (GC-FAME), Microbial ID, Newark, NY, 2006.
- [48] D.A. Hudman, N.J. Sargentini, Resazurin-based assay for screening bacteria for radiation sensitivity, *SpringerPlus* 2 (2013) 55.
- [49] S.D. Sarker, L. Nahar, Y. Kumarasamy, Microtitre plate-based antibacterial assay incorporating resazurin as an indicator of cell growth, and its application in the in vitro antibacterial screening of phytochemicals, *Methods* 42 (2007) 321–324.
- [50] C.F. Barbas, D.R. Burton, J.K. Scott, G.J. Silverman, Quantitation of DNA and RNA, Cold Spring Harb. Protoc. 2007 (2007) pdb. ip47.
- [51] Y. Iida, T. Tuziuti, K. Yasui, T. Kozuka, A. Towata, Protein release from yeast cells as an evaluation method of physical effects in ultrasonic field, *Ultrason. Sonochem.* 15 (2008) 995–1000.
- [52] W.E. Groves, F.C. Davis Jr., B.H. Sells, Spectrophotometric determination of microgram quantities of protein without nucleic acid interference, *Anal. Biochem.* 22

- (1968) 195–210.
- [53] H. Shi, G. Li, H. Sun, T. An, H. Zhao, P.-K. Wong, Visible-light-driven photocatalytic inactivation of *E. coli* by Ag/AgX-CNTs (X = Cl, Br, I) plasmonic photocatalysts: bacterial performance and deactivation mechanism, *Appl. Catal. B: Environ.* 158 (2014) 301–307.
- [54] A.J. Misra, S. Das, A.H. Rahman, B. Das, R. Jayabalan, S.K. Behera, M. Suar, A.J. Tamhankar, A. Mishra, C.S. Lundborg, Doped ZnO nanoparticles impregnated on Kaolinite (Clay): a reusable nanocomposite for photocatalytic disinfection of multidrug resistant *Enterobacter* sp. under visible light, *J. Colloid Interface Sci.* 530 (2018) 610–623.
- [55] G. Ferro, A. Fiorentino, M.C. Alferez, M.I. Polo-López, L. Rizzo, P. Fernández-Ibáñez, Urban wastewater disinfection for agricultural reuse: effect of solar driven AOPs in the inactivation of a multidrug resistant *E. Coli* strain, *Appl. Catal. B: Environ.* 178 (2015) 65–73.
- [56] P. Rai, S.M. Majhi, Y.T. Yu, J.H. Lee, Synthesis of plasmonic Ag@ SnO₂ core-shell nanoreactors for xylene detection, *RSC Adv.* 5 (23) (2015) 17653–17659.
- [57] R.J. Wu, D.J. Lin, M.R. Yu, M.H. Chen, H.F. Lai, Ag@ SnO₂ core-shell material for use in fast-response ethanol sensor at room operating temperature, *Sens. Actuators B: Chem.* 178 (2013) 185–191.
- [58] N. Zhang, S. Liu, Y.-J. Xu, Recent progress on metal core@ semiconductor shell nanocomposites as a promising type of photocatalyst, *Nanoscale* 4 (2012) 2227–2238.
- [59] R.M. Silverstein, G.C. Bassler, Spectrometric identification of organic compounds, *J. Chem. Educ.* 39 (1962) 546.
- [60] P. Van der Heide, X-Ray Photoelectron Spectroscopy, Wiley Online Library, 2011.
- [61] H. Chick, An investigation of the laws of disinfection, *Epidemiol. Infect.* 8 (1908) 92–158.
- [62] H.E. Watson, A note on the variation of the rate of disinfection with change in the concentration of the disinfectant, *Epidemiol. Infect.* 8 (1908) 536–542.
- [63] M. Castro-Alférez, M.I. Polo-López, P. Fernández-Ibáñez, Intracellular mechanisms of solar water disinfection, *Sci. Rep.* 6 (2016) 38145.
- [64] M.B. Keogh, M. Castro-Alférez, M. Polo-López, I.F. Calderero, Y. Al-Eryani, C. Joseph-Titus, B. Sawant, R. Dhodapkar, C. Mathur, K.G. McGuigan, Capability of 19-L polycarbonate plastic water cooler containers for efficient solar water disinfection (SODIS): field case studies in India, Bahrain and Spain, *Sol. Energy* 116 (2015) 1–11.
- [65] G. Carré, E. Hamon, S. Ennahar, M. Estner, M.-C. Lett, P. Horvatovich, J.-P. Gies, V. Keller, N. Keller, P. Andre, TiO₂ photocatalysis damages lipids and proteins in *Escherichia coli*, *Appl. Environ. Microbiol.* 80 (2014) 2573–2581.
- [66] S. Pigeot-Rémy, F. Simonet, E. Errazuriz-Cerda, J.C. Lazzaroni, D. Atlan, C. Guillard, Photocatalysis and disinfection of water: identification of potential bacterial targets, *Appl. Catal. B: Environ.* 104 (3-4) (2011) 390–398.
- [67] A. Russell, Bacterial resistance to disinfectants: present knowledge and future problems, *J. Hosp. Infect.* 43 (1999) S57–S68.
- [68] D. Li, S. Zeng, A.Z. Gu, M. He, H. Shi, Inactivation, reactivation and regrowth of indigenous bacteria in reclaimed water after chlorine disinfection of a municipal wastewater treatment plant, *J. Environ. Sci.* 25 (2013) 1319–1325.
- [69] M.E. Guerzoni, R. Lanciotti, P.S. Cocconelli, Alteration in cellular fatty acid composition as a response to salt, acid, oxidative and thermal stresses in *Lactobacillus helveticus*, *Microbiology* 147 (2001) 2255–2264.
- [70] A.N. Orekhov, E.A. Ivanova, Antithrombotic Efficacy of Nutraceuticals, Nutraceuticals, Elsevier, 2016, pp. 61–73.
- [71] J. Wong-Ekkabut, Z. Xu, W. Triampo, I.-M. Tang, D.P. Tielemans, L. Monticelli, Effect of lipid peroxidation on the properties of lipid bilayers: a molecular dynamics study, *Biophys. J.* 93 (2007) 4225–4236.
- [72] T.W. Ng, L. Zhang, J. Liu, G. Huang, W. Wang, P.K. Wong, Visible-light-driven photocatalytic inactivation of *Escherichia coli* by magnetic Fe₂O₃–AgBr, *Water Res.* 90 (2016) 111–118.
- [73] T. Leung, C. Chan, C. Hu, J. Yu, P. Wong, Photocatalytic disinfection of marine bacteria using fluorescent light, *Water Res.* 42 (2008) 4827–4837.
- [74] L. Rizzo, A. Fiorentino, A. Anselmo, Advanced treatment of urban wastewater by UV radiation: effect on antibiotics and antibiotic-resistant *E. Coli* strains, *Chemosphere* 92 (2013) 171–176.
- [75] A. Fiorentino, G. Ferro, M.C. Alferez, M.I. Polo-López, P. Fernández-Ibáñez, L. Rizzo, Inactivation and regrowth of multidrug resistant bacteria in urban wastewater after disinfection by solar-driven and chlorination processes, *J. Photochem. Photobiol. B: Biol.* 148 (2015) 43–50.
- [76] S. Rtimi, C. Pulgarin, J. Kiwi, Recent developments in accelerated antibacterial inactivation on 2D Cu-titania surfaces under indoor visible light, *Coatings* 7 (2017) 20.
- [77] L. Zheng, Y. Zheng, C. Chen, Y. Zhan, X. Lin, Q. Zheng, K. Wei, J. Zhu, Network structured SnO₂/ZnO heterojunction nanocatalyst with high photocatalytic activity, *Inorg. Chem.* 48 (5) (2009) 1819.
- [78] M. Sun, Q. Zhao, X. Liu, C. Du, Z. Liu, Comparative study on sandwich-structured SiO₂@Ag@SnO₂ and inverse SiO₂@SnO₂@Ag: key roles of shell ordering and interfacial contact in modulating the photocatalytic properties, *RSC Adv.* 5 (2015) 81059.